ELECTROPRODUCTION OF STRANGE NUCLEI*

E. V. HUNGERFORD†
Department of Physics, University of Houston,4800 Calhoun Rd,Houston TX 77204, USA
E-mail: Hunger@uh.edu

The advent of high-energy, CW-beams of electrons now allows electro-production and precision studies of nuclei containing hyperons. Previously, the injection of strangeness into a nucleus was accomplished using secondary beams of mesons, where beam quality and target thickness limited the missing mass resolution. We review here the theoretical description of the $(e, e'K^+)$ reaction mechanism, and discuss the first experiment demonstrating that this reaction can be used to precisely study the spectra of light hypernuclei. Future experiments based on similar techniques, are expected to attain even better resolutions and rates.

1 Introduction

It is generally understood that high energy electron scattering can illuminate the substructure of elementary hadronic particles, and even the more complicated quark/gluon substructure of nuclei. However it is less known, that electromagnetic reactions can also implant strange hadrons into nuclear matter, providing a new tool to precisely study the hadronic many-body problem.

Of course it is not possible, nor is it reasonable, to reproduce nuclear physics with strange hadrons. However the addition of strangeness into a nucleus adds a new degree of freedom which emphasizes questions impossible or difficult to address in non-strange nuclear systems. The discussion here will be developed in terms of quantum hadro-dynamics, where the interacting particles are the fundamental baryons and mesons having strangeness 0 or -1, although at some point in the future the quark substructure of nuclei may be required to adequately describe these systems[1].

Previously it has been established that a Lambda within a nucleus can be described as a distinguishable particle, moving in the nuclear mean-field[2]. In this representation a Lambda can reside deeply within the nuclear interior, interacting with the other hadrons near this position[3]. However one-pion-exchange with nucleons cannot occur due to isospin conservation, so the shorter range components of the hadronic interaction, including multi-pion exchange and $\Lambda - \Sigma$ coupling, are enhanced[4]. In addition, multi-strange nu-

*SUPPORTED IN PART BY THE US DOE
†FOR THE HNSS COLLABORATION AT THE JEFFERSON LABORATORY

clei are predicted to be particle stable, and neutron stars may contain equal numbers of strange and non-strange hadrons[5]. However as electromagnetic reactions effectively restrict strangeness changing reactions to Δ—S— = 1, we concentrate here only on the production and analysis of light Λ hypernuclei.

2 Electroproduction of Hypernuclei

The cross section for electroproduction can be written in a very intuitive form by separating out a factor, which under certain conditions, may be identified as the virtual photon flux produced by (e, e') scattering[6]. Using this notation the electroproduction cross section can be written;

$$\frac{\partial^3\sigma}{\partial \mathrm{E}'_e \partial\Omega'_e \partial\Omega_k} = \Gamma\left[\frac{\partial\sigma_T}{\partial\Omega_k} + \epsilon\frac{\partial\sigma_l}{\partial\Omega_k} + \epsilon\cos(2\phi) + \cos(\phi_k)\sqrt{2\epsilon(1+\epsilon)}\,\frac{\partial\sigma_I}{\partial\Omega_k}\right].$$

The factor, Γ, is the virtual flux factor evaluated for electron kinematics in the lab frame. It has the form;

$$\Gamma = \frac{\alpha}{2\pi^2\mathrm{Q}^2}\frac{\mathrm{E}_\gamma}{1-\epsilon}\frac{\mathrm{E}'_e}{\mathrm{E}_e}.$$

In the above equation, ϵ is the virtual photon polarization factor;

$$\epsilon = \left[1 + \frac{2|\mathbf{k}|^2}{\mathrm{Q}^2}\tan^2(\Theta_e/2)\right]^{-1};$$

which vanishes when the kaon is produced along the direction of the virtual gamma. The differential cross sections in the above expression are separated into transverse, longitudinal, polarized, and interference terms. For real photons of course, the 4-momentum (Q^2) vanishes, and only the transverse cross section is non-zero. In the production of strange nuclear systems, the kaon angle must be small in order to maintain a reasonable reaction rate, and for the experimental geometry described in this paper, $\mathrm{Q}^2 \rightarrow \frac{m_e^2\omega^2}{E_e E_{e'}}$. Therefore only the transverse cross section significantly contributes to the rate, and we approximate the electroproduction cross section by its on-shell value, *i.e.* by the (γ, K^+) cross section, so that the electro-production cross section is given by the virtual flux factor multiplied by the photo-production cross section[6].

2.1 The photo-production cross section

In order to describe the strangeness-producing reaction mechanism in a nucleus, we use the elementary process, $p(\gamma, K^+)\Lambda$, as was discussed above. The total cross section for this reaction was studied over a 1 GeV range above threshold[7]. The cross section rises from threshold at 0.91 GeV (photon energy) to a peak of 2.1 μb at 1.07 GeV. It remains nearly constant for about 0.5

GeV before gradually falling to about 1 μb at 1.9 GeV. Attempts have been made to describe this reaction in terms of an effective field theory, however there are no dominant Feynman diagrams as exist for pion photo-production, and many s,t, and u channel contributions must be included[8]. There are at least 10-15 undetermined coupling constants, and also a number of nucleon and hyperon resonances which must be included in any theory. Presently the data sample is inadequate to constrain the model, but quality data is now becoming available, and the situation may improve in the near future[9]. In any event, the forward-angle, unpolarized nuclear photo-production is insensitive to the details of the elementary amplitude.

In the laboratory frame the photo-production amplitude can be written in the general form[11];

$$\langle(\vec{k}-\vec{p}),\vec{p}|t|\vec{k},0\rangle = \epsilon_0(f_0 + g_0\sigma_0) + \epsilon_x(g_{-1}\sigma_1 + g_+\sigma{-}1).$$

Here ϵ is the photon polarization such that ϵ_z is perpendicular to the scattering plane and ϵ_x is along the incident photon direction. Then as the kaon production angle $\rightarrow 0$ we obtain;

$$\begin{aligned} f_0 &\rightarrow 0 \\ g_0 &\rightarrow a_1 \\ g_\pm &\rightarrow \pm\frac{a_1}{\sqrt{2}} \end{aligned}$$

This means that;

$$\langle(\vec{k}-\vec{p}),\vec{p}|t|\vec{k},0\rangle \rightarrow a_1\,(\vec{\sigma}\cdot\vec{\epsilon}).$$

2.2 The virtual Flux

The virtual flux factor rises very steeply to a maximum at an electron scattering angle of $\frac{m_e^2\omega^2}{E_eE_{e'}}$, Figure 1. For the energies involved here, this is very small, $\approx$ 2 milliradians, and falls to less than one-tenth its maximum value in 10 mr. Therefore if the electron spectrometer is placed at zero degrees, it need only have a small acceptance to assure that essentially all the scattered electrons are transported to the focal plane. This also means that aberrations in the optics of the magnetic transport system will be small, and easily corrected. The disadvantage of using the forward virtual flux is that bremsstrahlung also peaks in the forward direction and dominates the electron scattering process[6].

Therefore any attempt to observe a coincident reaction with zero degree virtual photons must cope with a large background of bremsstrahlung electrons.

Figure 1. The Virtual Flux Factor as a Function of the Electron Scattering angle

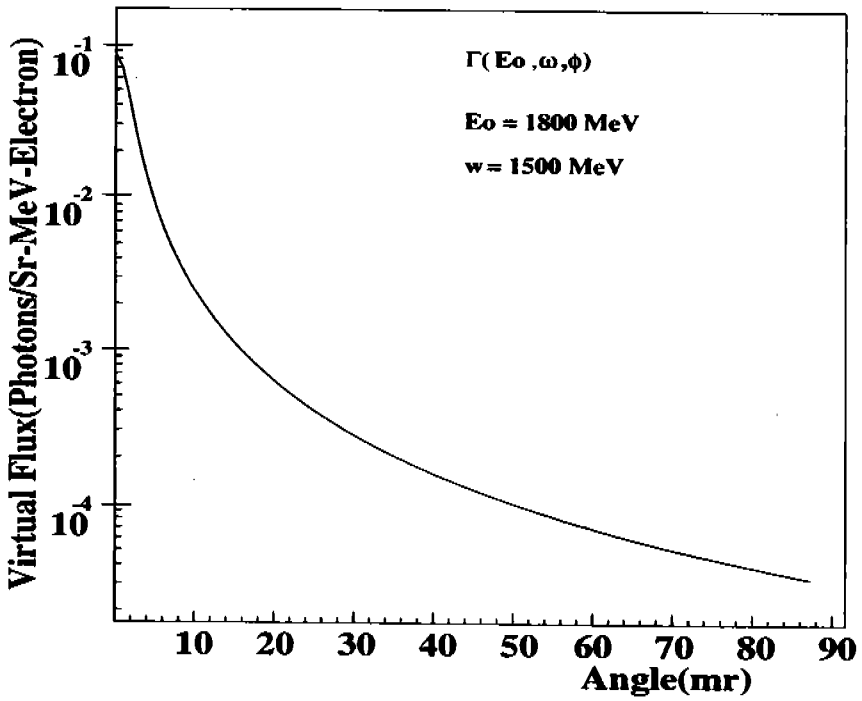

3 Photo-production of Strange Nuclei

The photo-production cross section on a nucleus can be written as[11];

$$\frac{d\sigma}{d\Omega} = \kappa |T_{ij}|^2$$

where the transition matrix, T_{ij} is;

$$T_{ij} = \frac{1}{2J_i + 1} \sum |\langle J_f m_f | O_{\gamma k} | J_i m_i \rangle|^2$$

and;

$$O_{\gamma k} = \int d^3x \, \chi_k^{-*} \chi_\gamma^+ \sum V \, \delta(r - \nu_v) \, \langle (\vec{k} - \vec{p}), \vec{p} | t | \vec{k}, 0 \rangle.$$

In this expression χ are the nuclear distorted waves, V is the transition matrix, $\delta(r - \nu v)$ is a recoil correction and the remaining term is the one-body

photo-production amplitude.

It has been demonstrated that the (γ, K^+) reaction mainly contains only the $\vec{\sigma} \cdot \vec{\epsilon}$ amplitude in the forward direction and that wave distortion decreases the cross section by perhaps 20% for light hypernuclei, leaving the angular distribution essentially unchanged[10].

4 Theoretical Expectations

Because of the spin dependence of the photo-production process, spin-flip transitions leading to non-natural parity hypernuclear states are favored. In addition because of the high momentum transfer of the (γ, K^+) reaction, high angular momentum transfer is also expected. This contrasts to mesonic production of hypernuclei, where natural parity states are preferentially populated. However the structure of the hypernuclear spectrum produced by all reaction processes is similar, owing to the weak spin dependence of the Λ-N interaction[11]. However, even though the shape of the spectra is similar, the spin structure of the unresolved states is completely different, and the strength of the transitions to the various hypernuclear states varies due to changes in the momentum transfer of the reactions.

Finally, based on the effective Λ-Nucleus interaction we expect that the $^{12}\mathrm{C}(\gamma, K^+)^{12}_{\Lambda}\mathrm{B}$ reaction will have s and p shell structure separated by approximately 11 MeV, and that there will be some small excitation of core excited states (nuclear excitations with the Λ in the s shell)[12].

5 Experimental Considerations

It is important to keep the incident electron beam energy below $\approx$ 1.8 GeV. A low beam momentum increases the experimental resolution, given a fixed $\Delta p/p$ in the spectrometer magnets, and minimizes the size of these magnets. In addition, it limits kaon production to elementary processes involving either Λs or Σs, as opposed to unwanted hyperon and meson resonances. Since the maximum hypernuclear photoproduction rate occurs at photon energies of about 1.5 GeV, the energy of the scattered electron would be 300 MeV in this case.

Strangeness production using either real or virtual photons, requires the associated production of a strange quark/anti-quark pair, and therefore one must detect multiple particles in the final state in order to undertake a kinematically complete experiment. Although strangeness production by mesons may also be associated, meson-induced reactions can be arranged so that only one particle need be measured in the final state, assuming of course, that the

momentum of the incident meson is determined. In addition, the rather high 3-momentum transfer, $\vec{q}$, for associated production is $\geq$ to the nuclear Fermi momentum. While this may be advantageous for the study of quark behavior, it decreases the probability of leaving a bound nuclear system in the final state. Thus the nuclear form factor, which falls rapidly with momentum transfer, essentially cuts off production of reaction particles at all but the very forward angles.

Thus, the greatest disadvantage of electroproduction is the requirement that both the electron and the K^+ must be detected in the restricted phase space region about the forward beam direction. To do this, the detection apparatus must consist of two momentum sensitive instruments placed at essentially the same forward-angle location, and having sufficient solid angle to capture a substantial fraction of the reaction particles.

The electron beam at the Jefferson National laboratory, Jlab, is ≈ 40 μm in diameter with a momentum dispersion of $\Delta p/p \approx 10^{-5}$. At a beam energy of $\sim$ 2 GeV, this introduces negligible error in the missing mass resolution. Beam stability is a much more important issue, i.e. the requirement that whatever the beam momentum, it must be stable and reproducible for days (weeks) during the course of an experimental run. In the experiment reported here, this was accomplished to a level of 10^{-4} by implementing momentum measurements in the beam arcs of the accelerator which were fed-back to the accelerator controls. In addition changes in beam momentum were recorded as each experimental run progressed and the data corrected for the momentum shift.

The layout of the HNSS (E89-009) experiment is shown in Figure 2. An electron beam of primary energy $\approx$ 1.8 GeV and $\sim$1 μA current strikes a thin target placed just before a small zero-degree dipole magnet. This magnet splits the scattered particles; the e^- of about 300 MeV/c into a split-pole spectrometer and the K^+ of about 1.2 GeV/c into the Short Orbit Spectrometer, SOS, fixed to the Hall C pivot at the Jefferson Laboratory. The magnetic optics of the splitting magnet/SOS system must be designed so that there is a virtual focus along the optic axis extension of the SOS magnet. In this case the image occurs somewhat further away than for a system without the splitting magnet, reducing slightly the acceptance, but preserving the optics. The splitting magnet is necessary in order to capture the scattered electrons and reaction kaons at very forward angles ($\leq 3°$). The resolution for the HNSS experimental arrangement is expected to approach 600 keV. Various contributions to this resolution are shown in Table 1, and are combined as if they were statistically independent. The system resolution is dominated by the SOS magnet, which is not designed for high resolution spectroscopy as

it has low dispersion and large momentum bite. However, it is a short-orbit magnet (important as the decay length for a 1.2 GeV/c kaon is about 9m), is already mounted and tested at the Hall C pivot, and has the sophisticated particle identification package, PID, required to extract kaons from the large background of pions and positrons.

Figure 2. The Experimental Geometry Showing the Zero Degree Splitting Magnet, the SOS Kaon Spectrometer, and the Enge Split-Pole Spectrometer.

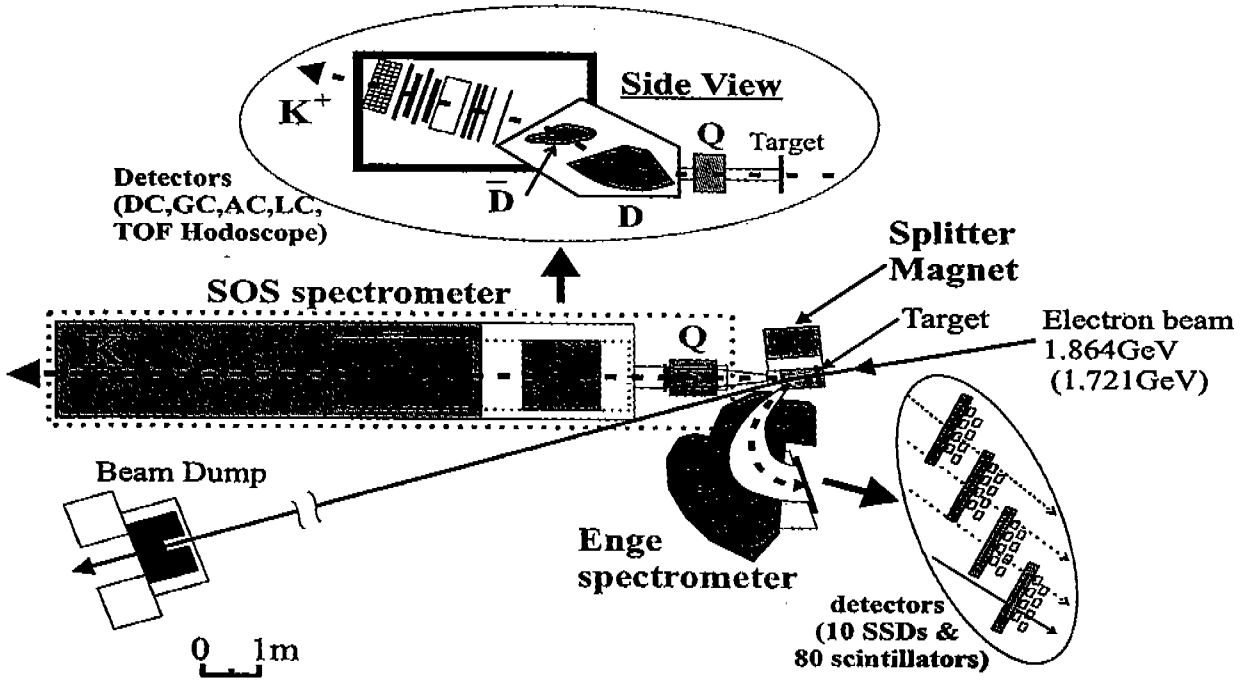

Nuclear targets, 22 mg/cm^2 of natural C and 10 mg/cm^2 of CH_2 were used. The CH_2 target was also used to observe Λ and Σ production from hydrogen and calibrate the missing mass spectrum. The reaction of interest, (e,e'K$^+$), resulted in the production of the $^{12}_{\Lambda}$B hypernucleus when C was the target. Beam intensities were tuned to produce an acceptable signal to accidental ratio, which in the unprocessed coincident-time spectrum was $\geq$ 0.2. For the C target this resulted in a current of approximately 0.6 μA, or an experimental luminosity of $\sim 3.5 \times 10^{33}$.

To satisfy the somewhat conflicting beam requirements of the different experimental Halls, the experiment was required to use two different beam energies, 1721 and 1864 MeV. Data analysis has shown that differences in the $^{12}_{\Lambda}$B spectra produced by these two beam energies were small. It was found that the reaction proton and pion flux dominated the kaons by several orders of magnitude.

Table 1. Anticipated Missing Mass Resolution in E89-009.

Component	Resolution Contribution (keV)
Splitter and Split-Pole Magnets	120
Beam	160
Splitter and SOS Magnets	550
Target	20
Scattering Angle Kinematics	200
Total	600

The electrons were detected near the focal plane of the Split-pole spectrometer by a set of silicon strip detectors (SSD). This detector package was specifically designed for the HNSS experiment to meet the spatial resolution and count-rate requirements. The SSD was backed by a scintillation hodoscope to provide timing signals. The coincident time resolution of this system was about 800 ps FWHM, and was sufficient to resolve the real and accidental time peaks in the 2 ns micro-structure of the Jlab beam. A set of 10 SSD boards covering a spatial range of 78 cm were used for the focal plane detector.

A spectrum with accidental background is shown in Figure 3. Clearly evident in the spectrum is ${}^{12}_{\Lambda}$B hypernuclear structure in which a Λ is inserted in the s and p shells at a B_Λ of -11 and 0, respectively. There also appears to be a core excited states between these peaks. The broad peak at about 38 MeV is due to Λ production from H in the CH_2 target, spread by the incorrect kinematics.

This spectrum is similar to that predicted by Motoba, *et al*[11] who indicated that the gs doublet is split by only 100 keV with the 2^- excited state receiving most of the strength. The resolution of the spectrum shown in Figure 3 is about 850 keV, and the spin structure of the major shells is not resolved. A discussion of the structure will require additional analysis, including the differential cross section scale.

6 Conclusions

The first HNSS experiment has successfully observed the electroproduction of ${}^{12}_{\Lambda}$B and collected data on the production of ${}^{7}_{\Lambda}$He. The missing mass resolution is consistent with the predicted value of 600 to 1000 keV, and is a factor of $\sim$ 3 better that existing measurements. The spectrum is also reasonably consistent with theory. Further analysis is expected to increase the statistics, and improve the backgrounds and resolution.

Figure 3. The Preliminary Hypernuclear Spectrum with Accidental Background. Clearly seen are the s and p shell excitations.

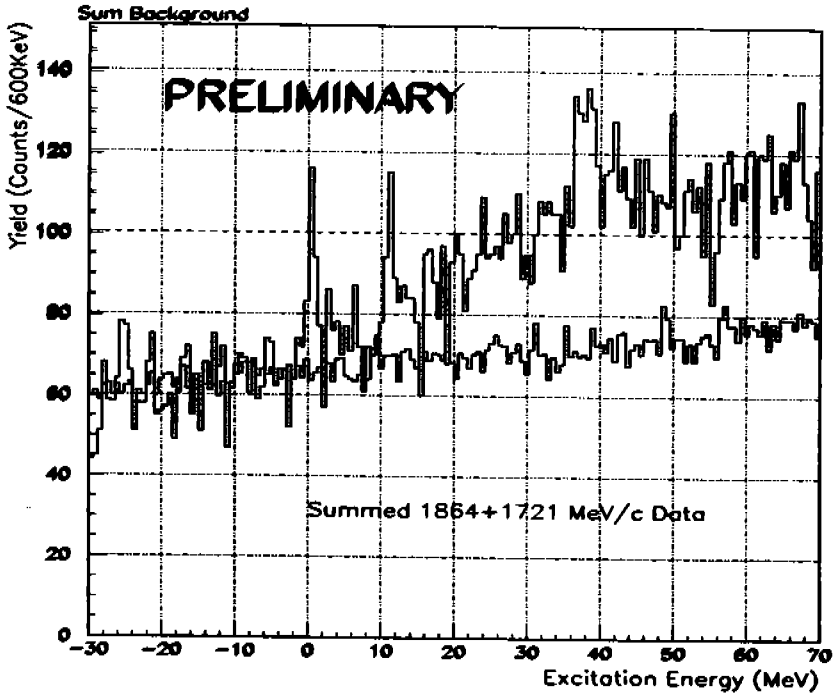

Targets for future experiments could consist of almost any separated-isotope of light mass since thicknesses of only $\approx$ 10mg/cm^2 are required. However as the target Z increases, electrons produced by bremsstrahlung processes increase as Z^2/A, but hyperon production increases as only as Z/A. Since bremsstrahlung limits the luminosity, the hypernuclear production rate should fall as $1/Z$. Of course nuclear effects must be applied, but from this analysis the HNSS geometry is suitable for lighter, p-shell targets. A newly designed geometry[13] with a specially constructed kaon spectrometer is planned which will allow extension of these studies well beyond the p-shell. This new system could improve the resolution by a factor of 2, with a increase in rate by a factor of as much as 50.

References

1. K. Maltman and M. Shmatikov, Nucl. Phys. **A585**(1995)343c; E. V. Hungerford and L. C. Biedenharn, Phys. Lett. **142B**(1984)232.
2. D. J. Millener, A. Gal, and C. B. Dover, Phys. Rev. **C38**(1988)2700.
3. H. Feshbach, *Proceedings of the Summer Study Meeting on Nuclear and Hypernuclear Physics with Kaon Beams*, H. Palevsky, ed. BNL Report

18335, July 1973.
4. B. F. Gibson and E. V. Hungerford, Phys. Rep., **257**(1995)350.
5. H. Bethe, G. E. Brown, and J. Cooperstein, Nucl. Phys. **A462**(1987)791; M. Prakish, *et. al.*, Phys. Rev. **D52**(1994)661; N. K. Glendenning and S. A. Moszkowski, Phys. Rev. Lett. **67**(1991)2414, N. Glendenning, Phys. Rev. **64C**(2001)025801.
6. Jlab experiment 89-009 and related documents, E. Hungerford, spokesperson, E. V. Hungerford, Prog. Theor. Phys. Sup. **117**(1994)135; Proceedings of the APCTP Workshop(SNP'99), IL-T. Cheon, S. W. Hong, and T. Motoba, eds, World Scientific, Singapore, 2000.
7. B. Saghai, Jlab Workshop on Electroproduction of Strangeness in Nuclei, December, 1999, Hampton University; B. Saghai, Euro. Jou. Phys. **C15**(2001).
8. M. Mart and C. Bennhold, Phys. Rev. **C61**(1999); C. Bennhold, Jlab Workshop on Electroproduction of Strangeness in Nuclei, December, 1999, Hampton University.
9. see the large numbers of papers presented at this conference.
10. R. A. Adelseck, *et al*, Ann. of Phys. **184**(1988)33; O. Richter, M. Sotona, and J. Zofka, Phys. Rev. **C43**(1991)2753
11. T. Motoba, M. Sotona, and K. Itonaga, Prog. Theor. Phys. **117**(1994)123; M. Motoba, *et al*, Prog. Theor. Phys. Sup. **117**(1994)135; M. Sotona and S. Frulani, *et al*, Prog. Theor. Phys. Sup. **117**(1994)135.
12. D. J. Millener, Nucl. Phys. **A691**(2001)93c.
13. O. Hashimoto, this conference, private communication, Jlab experiment 97-008.